PHYSICAL REVIEW A **89**, 042503 (2014)

Relativistic configuration interaction calculations for some two- and three-electron systems with screened hydrogenic spin orbitals

Leszek Głowacki and Jacek Migdałek[*]
Department of Computer Science and Computer Methods, Pedagogical University of Cracow, Podchorążych 2, 30-084 Kraków, Poland

(Received 27 November 2013; published 7 April 2014)

An approach is proposed for the generation of virtual spin orbitals required to construct a configuration state function basis set for relativistic configuration interaction calculations. Screened hydrogenic spin orbitals, corresponding to noninteger nuclear numbers determined separately for each orbital employing the so-called condensed-space concept are proposed and used here. To test the method calculations are performed of ionization and transition energies of two- and three-electron systems such as He, He-like Ne and He-like U, Li, Li-like Ne and Li-like U, including Breit interaction and quantum electrodynamic corrections.

DOI: 10.1103/PhysRevA.89.042503 PACS number(s): 31.15.am, 31.15.ag

I. INTRODUCTION

The knowledge of atomic structure data such as energy levels, transition probabilities, and lifetimes is still important for laboratory and astrophysical plasma diagnostics, construction of new light sources, atomic clocks, as well as atomic and ionic manipulation for quantum information transformation. Contemporary calculation tools in popular use are the relativistic multiconfiguration Dirac-Fock method (MCDF) [1,2] and the configuration interaction Dirac-Fock approach (CIDF). The first method includes determination of both spin orbitals and coefficients needed to construct multiconfiguration wave functions in subsequent double iterative self-consistent field processes in order to minimize the energy of required level (optimal level, OL scheme) or chosen average of levels (average level, AL scheme). This approach is the most efficient known so far if one accepts the full separation of variables in the many-electron wave function. However, with the use of a reasonably long configuration state function (CSF) basis set, such procedure is still plagued by convergence problems of the iterative process. Therefore the most often used alternative is the configuration interaction approach, where only the spin orbitals are determined in a self-consistent field iterative process and configuration interaction coefficients are computed in a single energy matrix diagonalization procedure. The main inconvenience in this case is the need to use a large basis set to represent electron correlation effects, particularly when spectroscopic spin orbitals are used as correlating virtual, i.e., unoccupied orbitals. It had been observed a long time ago that correlating orbitals obtained in fully multiconfiguration procedures are much more contracted in comparison with their spectroscopic counterparts. For instance the correlating orbital in Be obtained in MCHF calculation is much more close to the orbital of Be^+ ion than to its spectroscopic counterpart [3,4]. The use of appropriate correlating orbitals largely improves the efficiency of the CI scheme to represent electron correlation effects. Therefore in the past few years we had tried to explore different methods to generate the virtual spin orbitals in the field of an *ab initio* model potential in order to use them in CI procedure [3–5]. This idea turned out to be successful in many cases, particularly when the core-valence electron correlation dominates over the intravalence or core-core correlation. However in our opinion there is still a need to develop a more general approach to problems of construction spin orbitals to improve the efficiency of the CI scheme. We found that each correlated spin orbital feels different attraction by the nucleus. This enabled us to use hydrogenic spin orbitals corresponding to noninteger atomic numbers. Of course such orbitals are too contracted in comparison, for example, with those obtained by the MCDF approach. But this inconvenience should be corrected by the greater contribution of higher excited spin orbitals. It is supposed here that the lower the excited spin orbital, the lower the noninteger nucleus charge is affecting it. In that sense the lower excited spin orbitals are screened. On the other hand, the higher the excited virtual spin orbitals are, the greater is their ability to penetrate the region near the nucleus.

In this paper we propose an approach and test it in computation of energies of two- and three-electron systems such as He, He-like Ne, He-like U and Li, Li-like Ne and Li-like U.

II. CALCULATIONS

A. Generation of spin orbitals; concept of condensed space transformation of energy levels

The presented method is based on an assumption that there exists a space of energy states for charged particles called by us Q space. Q space is assumed to be countable, which means that all states can be numbered. The states in Q space can be interpreted as energy levels occupied by the charged particles. They are denoted by $|q\rangle$ where q is the integer number. Let us introduce subspace E as a set of energy states and assume that all the other states in Q space are completely filled. The ground state of the E space is always denoted as $|1\rangle$. The remaining states are designated by the q-integer numbers in order of their positions. If some states are filled the proper levels will be omitted. We can also introduce the $\hat{Z}$ operator, which acts in the E space representing a charge affecting the particle being in particular state. It can be associated with the eigenvalue equation

$$\hat{Z}|q\rangle = Z_q|q\rangle. \tag{1}$$

---

[*] lg@up.krakow.pl

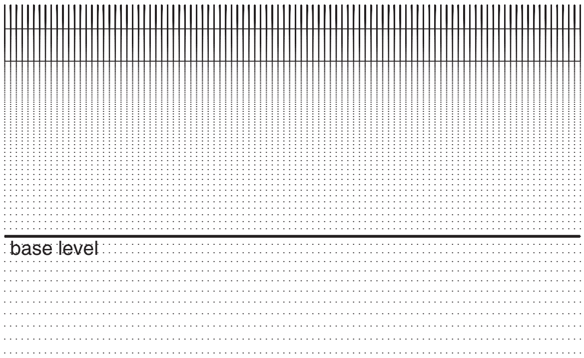

FIG. 1. The model of E space for the hydrogen atom in nonrelativistic approximation. The horizontal dotted lines represent filled states of the space. The solid lines represent spectroscopic states. The base level represents here the ground level

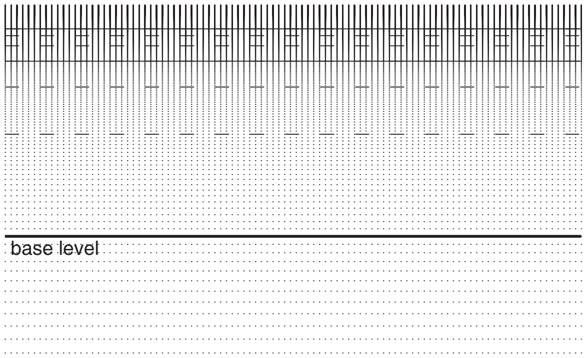

FIG. 2. Condensed $E^{(s)}$ space of degree $s = 2$. The base level represents here the ground level. The dashed lines represent virtual states. The solid lines except for base level also represent virtual states in that space. Note that solid lines correspond to the spectroscopic states in original E space.

The eigenvalues Z_q assume real positive values. The representation of the $|q\rangle$ states in Q space is the hydrogenlike wave functions with $Z = Z_q$ and $n = q$ principle quantum number. The states of particles corresponding to the integer Z_q eigenvalues are called spectroscopic, i.e., they can be observed. Let us consider the E space as a set of energy states of a hydrogen atom in Schrödinger approximation. The energy levels can be evaluated in a.u. from

$$\epsilon_n = -\frac{1}{2n^2}, \tag{2}$$

where n is the integer principle quantum number. Since all eigenvalues of the $\hat{Z}$ operator in this space are equal to 1 all states are spectroscopic. Now let us perform a transformation denoted by $\epsilon_s \to \epsilon_1$, which moves the position of one of the excited energy levels ϵ_s into the place originally occupied by the ground level ϵ_1. It can simply be done by increasing the atomic charge. In result all other levels change its position creating new $E^{(s)}$ space. The level denoted here by ϵ_1 is called base level. We arbitrarily assume that such transformation cannot create new states lying under the base level in the $E^{(s)}$ space. This means that two spaces E and $E^{(s)}$ have the same ground level. It has fundamental meaning for the conception of condensed space. The possible explanation of this fact may be done in terms of quantum dynamics theory. We suppose that during the transformation of the E space into $E^{(s)}$ the virtual positron-electron pairs are created from which the electrons move under the base level and positrons move above the base level. As a consequence all states under the base level are being kept filled and above the base level the virtual states are produced. It is interesting to note that all spectroscopic levels also remain unchanged. But, in the $E^{(s)}$ space some new levels emerge between the spectroscopic levels. The pictures of two spaces E and $E^{(s)}$ are illustrated in Figs. 1 and 2. The space E in Fig. 1 represents here the Coulomb potential in a hydrogen atom but $E^{(s)}$ on Fig. 2 corresponds to some different potential, which might even not be expressed analytic form. All levels in the $E^{(s)}$ space except base level correspond to noninteger eigenvalues of the $\hat{Z}$ operator, therefore we can call them virtual levels. The eigenvalues of the $\hat{Z}$ operator in that space can be evaluated from the formula

$$Z_q = \frac{q(s+b)}{b(s+q)}, \tag{3}$$

with the integer parameters $b = 1$ and $q \geqslant 1$. States named $|(s+1)q\rangle$ correspond to the spectroscopic states of the E space. If we allow for all virtual states in the $E^{(s)}$ space to be filled then the only accessible states are the spectroscopic states and this leads back to the spectroscopic E space. Thus the spectroscopic space of energy levels can be treated as a subspace of Q having all its virtual states filled.

The transformation described above is called by us a condensed-space transformation, which may be also interpreted as creating a charge operation. We denote such transformation by $\epsilon_s \to \epsilon_b$, where the b parameter is the principal quantum number of the state associated with so-called base level (which in general does not need to be the ground level) and $s \geqslant 0$ is the integer parameter. The base level must correspond to some of the existing spectroscopic state. This transformation acts in Q space. It transforms the $E \subset Q$ space into the $E^{(s)} \subset Q$ space. We assume that $E^{(0)} \equiv E$. The representation of the $|q\rangle$ states belonging to the $E^{(s)}$ space is the hydrogenlike wave functions with $Z = Z_q$ and $n = q$. The Z_q eigenvalues of the $\hat{Z}$ operator can be evaluated from the formula (3). The transformation creates new virtual states above base level in the $E^{(s)}$ space (Fig. 2). Both E and $E^{(s)}$ spaces have the common states with $q \leqslant b$. The transformation cannot change the spectroscopic energy levels of the original E space although they may correspond to different states in the $E^{(s)}$ space. In the model of quantum dynamics electrons interact with each other via exchange of virtual photons. Thus in our opinion the model of condensed space should be adequate to reproduce e-e interactions in the relativistic configuration interaction scheme.

In our CI calculations the basis set is constructed using a finite $E^{(s)}$ subspace of virtual states. For such subspace we can define quantity ρ by

$$\rho = \frac{1}{|\epsilon_b - \epsilon_m|}, \tag{4}$$

as a density of space. An integer m is the size of the chosen subspace of $E^{(s)}$. The density of subspace can be enlarged by increasing the integer parameter s. Taking CI calculations into account the largest ρ should be provided. In the relativistic approach the spectroscopic E space should be created by the states of the hydrogenlike ion in Dirac-Coulomb approximation. The energy levels depend here on two quantum numbers. The proper condensed-space transformation that preserves the spectroscopic states can be written as $\epsilon_{b+s,1+s} \rightarrow \epsilon_{b,1}$. The base level depends on the integer b principle quantum number and the $|\kappa| = 1$ quantum number associated with electron total angular momentum. We can find that $|(s+1)n,(s+1)|\kappa|\rangle$ states correspond to the spectroscopic states in the E space. The eigenvalues of the $\hat{Z}$ operator can be obtained as solutions to

$$\frac{A(s+1)}{(s+1)\sqrt{1-(\alpha A)^2}+n-|\kappa|+s(b-1)} = \frac{Z_{n,\kappa}}{\sqrt{\kappa^2-(\alpha Z_{n,\kappa})^2}+n-|\kappa|}, \tag{5}$$

where A is atomic number, α fine structure constant, and with $n \geqslant b, |\kappa| \leqslant n$ the integer quantum numbers. Equation (5) is the relativistic form of Eq. (3). The ρ density of the $E^{(s)}$ condensed space increases with the integer parameter s, which therefore it can be interpreted as a degree of condensation. As we mentioned earlier the larger the value of s, the more virtual states occur in the $E^{(s)}$ space and consequently this yields the better reproduction of the electron-electron interaction. However one can note that for large enough value of the parameter s and particularly for heavy systems, some states, especially with $|\kappa| = 1$, may not have the real eigenvalues of the $\hat{Z}$ operator due to the singularity in Eq. (5). Thus the magnitude of the s parameter may be increasing until this singularity occurs. This may happen especially for higher excited virtual states in strongly ionized systems. As we see, in the relativistic approach the degree of condensation of E space is limited.

We employed the $E^{(s)}$ space in our relativistic configuration interaction calculations assuming that it represents all possible states that may be occupied by the charged particles. The value of the s parameter in Eq. (5) was chosen as high as possible. The b parameter in Eq. (5), which corresponds to base level in $E^{(s)}$ space was determined as the principal quantum number of the outermost orbital in the ground-state configuration of the system studied. Since the virtual states under the base level are filled, the one-particle states of the ground-state configuration are treated in the $E^{(s)}$ space as the spectroscopic states. The wave functions of these states were determined as the hydrogenlike wave functions in Dirac-Coulomb approximation. The wave functions of the virtual states satisfied the one-electron Dirac-Coulomb eigenequations

$$\left(c\alpha \cdot \hat{p} + mc^2\beta - \frac{Z_{n,\kappa}}{r}\right)\phi_{n,\kappa} = \epsilon\phi_{n,\kappa}, \tag{6}$$

where the $Z_{n,\kappa}$ parameters were evaluated as the eigenvalues of the $\hat{Z}$ operator in the $E^{(s)}$ condensed-space. We used the orthogonal basis $\phi_{n,\kappa}$ in CI calculations. One can note that such scheme of generation of wave functions enabled us to use the same set of spin orbitals in CI calculations for all states of the system under consideration.

B. Relativistic configuration interaction (RCI) scheme

A many-body Hamiltonian most commonly used for atomic structure calculations is the relativistic Dirac-Coulomb Hamiltonian, which is given by

$$H^{DC} = \sum_i h_D(i) + \sum_{i<j} \frac{1}{r_{ij}}, \tag{7}$$

where h_D is the one-electron Dirac Hamiltonian and $1/r_{ij}$ represents the nonrelativistic Coulomb repulsion between two electrons. The relativistic correction to the Coulomb repulsion, which is known as Breit interaction

$$B_{ij} = -\frac{\alpha_j \cdot \alpha_j}{r_{ij}} \cos(\omega_{ij} \cdot r_{ij}) + \alpha_i \nabla_i \cdot \alpha_j \nabla_j \left[\frac{\cos(\omega_{ij} \cdot r_{ij}) - 1}{\omega_{ij}^2 \cdot r_{ij}}\right] \tag{8}$$

included in the electron-electron Coulomb interaction yields the Dirac-Coulomb-Breit Hamiltonian

$$H^{\mathrm{DCB}} = \sum_i h_D(i) + \sum_{i<j}\left(\frac{1}{r_{ij}} + B_{ij}\right). \tag{9}$$

The variable ω [Eq. (8)] is defined here

$$\omega_{ij} = (\epsilon_i - \epsilon_k) \cdot \alpha \tag{10}$$

as the frequency of the virtual photon exchanged between interacting electrons, where α is the fine-structure constant. In our approach the quantity ϵ_i considered as the level from the condensed space of energy levels leads to

$$|\omega_{ij}| \leqslant \frac{1}{\rho}, \tag{11}$$

where ρ is the density of condensed space defined above. It is interesting to note that enlargement of the density ρ leads to decrease the frequency ω in the Breit term of the Hamiltonian. Since the largest density ρ can be achieved only for neutral or light ionized atoms, the Breit interaction term can be reduced here to its limiting static form

$$B_{ij}(0) = -\frac{\alpha_i \cdot \alpha_j}{2r_{ij}} - \frac{(\alpha_i \cdot \mathbf{r_{ij}})(\alpha_j \cdot \mathbf{r_{ij}})}{2r_{ij}^3}, \tag{12}$$

the so-called frequency-independent Breit operator. For highly ionized systems the density ρ must be considerably smaller due to singularity of Dirac equation eigenenergies for $s_{1/2}$ or $p_{1/2}$ states (as discussed in Sec. II A) and in consequence the frequency-dependent Breit operator should be applied in such systems.

The present calculations employ both the Dirac-Coulomb (DC) as well as Dirac-Coulomb-Breit (DCB) Hamiltonian. To avoid the problem of variational collapse the basis set expansion of CSF should be restricted to electron states. In this study the projection onto electron states was achieved by using positive energy hydrogenic spin orbitals as basis functions which were solutions of Eq. (6). The electron correlation effects included here are represented by single, double, and for a system with three electrons, also triple excitations from

TABLE I. Comparison of CI calculations using screened hydrogenic (SH) basis and H-like basis.

Method	He ground state ionization energy (ev)	Excitation energy of $1s2p\,{}^3P_1$ in He (cm^{-1})
CI(H-like $Z = 2$)	23.7408(1235 no. CSF)	165655 (3150 no. CSF)
CI(H-like $Z = 8$)	24.4714(1235 no. CSF)	168527 (3150 no. CSF)
CI(SH)	24.5863(1235 no. CSF)	169055 (3150 no. CSF)
Experiment	24.587387[a]	169086.8[b]

[a] Reference [7].

[b] Reference [8].

the reference configuration. The excitation range depended on the system under consideration and for helium reached $n = 60$ with $l \leqslant 5$ whereas for lithium it was $n = 15$–30 and $l \leqslant 3$. For heliumlike ions the corresponding range of quantum numbers were $n \leqslant 25$ and $l \leqslant 5$, whereas for lithiumlike systems $n \leqslant 20$ and $l \leqslant 3$.

The construction of configuration state function (CSF) space was performed in two steps. First, the large sparse Hamiltonian matrix was evaluated as complete CI expansion as possible. The off-diagonal matrix elements were evaluated only for configurations built as the single excitations from the reference configuration. It means that the off-diagonal sparse-matrix elements, which involved the pair of configurations being double or triple excitations from the reference configuration were neglected. The sparse matrix included 2300–42350 CSF for helium and 100 000–700 000 for lithium. The configurations' expansion coefficients resulting from the diagonalization of the sparse matrix were later used to select configurations with large enough contributions, i.e., with mixing coefficients greater than 10^{-5} or 10^{-6}. This enabled us to construct the so-called dense matrix, from which all off-diagonal elements for selected configurations were evaluated. In the most cases the order of the matrix ranged from 1500–17000 CSF depending on the system under consideration.

TABLE II. Ionization energies (in eV) of some levels of helium, heliumlike neon (Ne^{+8}) and heliumlike uranium (U^{+90}) computed in this study [RCI(SH)] in Dirac-Coulomb (DC), Dirac-Coulomb-Breit (frequency-independent) [DCB(0)], Dirac-Coulomb-Breit (frequency-dependent) [DCB(ω)] approximations with and without QED corrections.

	He ($1s^2\,{}^1S_0$)	
RCI(SH), DCB(0) + QED[a]		24.587618
Experiment[d]		24.587387
	Ne^{+8}($1s2p\,{}^3P_0$)	
	DC	DCB(0)
RCI(SH)[b]	281.15419	281.04649
RCI[e]	281.15422	281.04652
MBPT[f]	281.15425	281.04657
	U^{+90}($1s^2\,{}^1S_0$)	
RCI(SH), DCB(ω) + QED[c]		129568.2
Artemyev et al.[g]		129570.3(6)

[a] Basis set expansion: $58s58p58d58f58g58h$, number of selected CSF 12726.

[b] Basis set expansion: $20s20p20d20f20g20h$, number of selected CSF 1696.

[c] Basis set expansion: $20s20p20d20f20g20h$, number of selected CSF 759.

[d] Reference [7].

[e] Reference [9].

[f] Reference [10].

[g] Reference [11].

Ionization and transition energies as well as correlation energy contributions have been computed for helium, heliumlike neon and heliumlike uranium, lithium and lithiumlike neon, and lithiumlike uranium including Breit frequency-independent [$B(0)$] and frequency-dependent [$B(\omega)$] contribution with and without QED corrections.

For highly ionized systems such as heliumlike uranium the quantum mechanics (QED) effects become very strong. However it is not possible to do a full QED treatment as a part of relativistic Hamiltonian. In our calculations the dominant QED corrections (self-energy, vacuum polarization) referred as a Lamb shift were evaluated in perturbative way. This means that total QED corrections to many-electron atoms or ions were given by a sum of one-electron QED contributions weighted by effective occupation number of each spin orbital as obtained form the eigenvectors of CI-DCB calculations. The most important one-electron self-energy contributions were calculated using the method developed by Mohr [6] and the screened self-energy was obtained using the model based on the ratio of the electron charge densities near the nucleus. Three leading contributions to vacuum polarization of orders: $\alpha(Z\alpha)$, $\alpha(Z\alpha)^3$, $\alpha^2(Z\alpha)$ were included in the Lamb shift. The strongest effect near the nucleus, besides the relativistic one, comes from extended nuclear charge density. We used the finite nuclear model with uniform spherical charge for the nuclei of light ($Z \leqslant 45$) and Fermi (with a thickness parameter 2.3 fm) distribution for heavy atoms. The finite nuclear size correction to the self-energy were also taken into account in our DCB + QED calculations.

III. DISCUSSION OF RESULTS

In order to compare our CI approach with original CI using the H-like basis we performed calculations of the ground-state ionization energy in neutral helium and the excitation energy of its excited state. The calculations were done with the nonrelativistic approach (i.e., assumed speed of light was 10^6). The original CI approach used the virtual H-like basis with $Z = 2$. We found also that the H-like $Z = 8$ basis yielded the best result of ionization energy. For comparison we took both results. The obtained results are presented in Table I. Comparing to experiment both the ground-state ionization energy and the excitation energy of $1s2p\,{}^3P_1$ state in neutral

TABLE III. Excitation energies (in cm^{-1}) (vs the ground state) of energy levels in neutral helium calculated with RCI(SH) method in Dirac-Coulomb approximation.

Level	Present results[a]	Experiment[b]
$1s2p\,^3P_1$	169074.1	169086.8
$^1P_1$	171121.7	171134.9
$1s3p\,^3P_1$	185550.7	185564.6
$^1P_1$	186195.4	186209.4
$1s4p\,^3P_1$	191200.0	191217.8
$^1P_1$	191474.3	191492.7
$1s5p\,^3P_1$	193809.9	193800.7
$^1P_1$	193968.7	193942.5

[a] Basis set:$55s55p55d55f55g55h$, number of selected CSF for $^1P_1$, $^3P_1$:10880 and for $^1S_0$:8229.

[b] Reference [8].

helium we can see that CI with screened hydrogenic spin orbitals yielded the best results. Note that using the H-like basis with $Z = 8$ the original CI approach needed 1235 of CSF to yield the value 24.47 eV for helium ionization energy. This level of accuracy was reached by our approach with only 16 of selected CSF included in the basis set. We can see great advantage of using screened-hydrogenic orbitals in comparison with other H-like bases.

The results of present calculations [RCI(SH)] obtained for two- and three-electron systems are presented in Tables II and III respectively and compared with other theoretical and experimental data available. System and levels have been chosen for consideration because of availability of other data that could be used for comparison. All tables presented here contain also information concerning the basis set expansion and number of configuration state functions (CSF) used in given calculations.

As can be seen from Table II the relative agreement of ground-state $1s^2\,^1S_0$ correlation energy with experiment is for He and U^{+90} better than 0.002%. Our results agree very well also with other available theoretical data. For $1s2p\,^3P_0$ ionization energy in Ne^{+8} there is no experimental value available but the agreement of our and other theoretical data for both Dirac-Coulomb and Dirac-Coulomb-Breit (frequency-independent) approximations is also very good. The slight differences could be due to neglecting of the higher l states in the basis set of our calculations, which were taken into account in RCI [9] and MBPT [10]. We have also calculated in DCB(0) + QED approximation first (vs $1s^2\,2s\,^2S_{1/2}$ ground state) and second (vs $1s^2\,^1S_0$ ground state of Li$^+$) ionization potential for neutral lithium. The basis set expansion of $45s45p45d45f45g45h$ orbitals included 220038 selected CSF. The obtained results: 5.39085 eV and 75.6397 eV agree very well with the corresponding experimental data: 5.391715 eV [12] and 75.6400 eV [13], respectively.

Table III presents excitation energies of some levels of neutral helium computed in the present study in Dirac-Coulomb approximation with available experimental data. The relative agreement in all (except one) cases is better than 0.01%. Slightly worse accuracy here is caused by the greater difficulty in precise theoretical determination of excited states.

TABLE IV. Transition energies (in eV) for $1s^22s\,^2S_{1/2} - 1s^22p\,^2P_{1/2,3/2}$ transitions in neutral lithium (Li), lithiumlike neon (Ne^{+7}), and uranium (U^{+89}) calculated in Dirac-Coulomb (DC), Dirac-Coulomb-Breit (frequency-independent) [DCB(0)], Dirac-Coulomb-Breit (frequency-dependent) [DCB(ω)] approximations with and without QED corrections.

Method	Transition energy $^2S_{1/2} - {}^2P_{1/2}$	Transition energy $^2S_{1/2} - {}^2P_{3/2}$
	Li	
RCI(SH)[a], DC	1.848129	1.848187
RCI(SH), DCB(0)	1.848070	1.848112
Experiment[d]	1.847818	1.847860
	Ne^{+7}	
RCI(SH)[b], DC	15.8935	16.1193
RCI(SH), DCB(0)	15.9111	16.1145
RCI(SH), DCB(0) + QED	15.8888	16.0933
RCI[e]	15.8888	16.0933
MBPT[f]	15.8885	16.0931
Experiment[e]	15.8887(2)	16.0932(2)
	U^{+89}	
RCI(SH)[c], DC	286.145	4514.41
RCI(SH), DCB(0)	322.52	4505.16
RCI(SH), DCB(ω)	322.15	4498.06
RCI(SH), DCB(0) + QED	280.86	4465.70
RCI(SH), DCB(ω) + QED	280.49	4458.60
RCI[g], DC	–	4514.79
RCI[g], DCB	–	4498.87
MBPT[f], DC	286.145	4514.81
MBPT[f], DCB(0)	322.75	4505.62
MBPT[f], DCB(ω)	322.38	4498.56
Experiment[h]	280.59(10)	4459.37(21)

[a] Basis set expansion: $15s15p15d15f$, number of selected CSF for $^2P_{3/2}$,$^2P_{1/2}$,$^2S_{1/2}$: 33750, 20865, and 19345 respectively.

[b] Basis set expansions for $^2S_{1/2} - {}^2P_{3/2}$ calculations: $13s13p13d13f$, number of selected CSF: 4062, 5849 respectively and for $^2S_{1/2}$-$^2P_{1/2}$ calculations: $15s15p15d15f$, number of selected CSF: 5045, 4781 respectively.

[c] Basis set expansion: $17s17p17d17f$, number of selected CSF for $^2P_{3/2}$,$^2P_{1/2}$,$^2S_{1/2}$: 6655, 4768, and 4645 respectively.

[d] Reference [15].

[e] Reference [16].

[f] Reference [17].

[g] Reference [18].

[h] References [19,20].

Table IV shows $1s^22s\,^2S_{1/2}$–$1s^22p\,^2P_{1/2,3/2}$ transition energies computed here for three-electron systems (Li, Ne^{+7}, U^{+89}) compared with other theoretical and experimental data available. The RCI(SH) calculations were performed with the basis set expansions included single, double, and triple excitations from the ground-state configuration. In the case of neutral lithium the CSF were selected to those with mixing coefficients greater than 10^{-8}. Our Dirac-Coulomb-Breit results for neutral lithium after subtraction of corrections from reduced mass and mass polarization (0.000245 eV taken from Ref. [14]) yield 1.847825 eV and 1.847867 eV for $^2S_{1/2}$-$^2P_{1/2}$ and $^2S_{1/2}$-$^2P_{3/2}$ transitions respectively, and are in excellent agreement with experimental data. The agreement

TABLE V. Comparison of frequency-independent [B(0)] and frequency-dependent B(ω) Breit contribution as well as the Lamb shift computed for some transition energies in lithiumlike uranium with results of other theoretical methods (in eV).

Method	Transition $^2S_{1/2}-{}^2P_{1/2}$	 $^2S_{1/2}-{}^2P_{3/2}$
	Breit contribution	
RCI(SH), DCB(0)	36.37	−9.25
RCI(SH), DCB(ω)	−0.37	−7.10
MBPT[a], DCB(0)	36.60	−9.16
MBPT, DCB(ω)	−0.37	−7.06
	Lamb shift	
RCI(SH)	−39.46	−41.66
other theory	−39.13(5)[b]	−41.68(5)[c] −41.77[d]

[a] Reference [17].
[b] Extrapolated from Blundell's results of [21] for $Z = 60, 70, 80, 90$.
[c] Reference [21].
[d] Reference [22].

with experiment of our other theoretical results is very good, particularly if, at least, the Breit frequency-independent term $[B(0)]$ and QED corrections are included in calculations. One can note clear importance of QED corrections whereas the Breit frequency-dependent term $[B(\omega)]$ plays visible role only for $^2S_{1/2}$–$^2P_{3/2}$ transition.

Table V presents contributions of the Breit interaction [both $B(0)$ and $B(\omega)$] and of the Lamb shift to $1s^22s\,{}^2S_{1/2}$–$1s^22p\,{}^2P_{1/2,3/2}$ transition energies in Li-like U computed in this study and compared with other theoretical results. As can be seen, the contribution of the frequency-independent Breit interaction $[B(0)]$ is for $^2S_{1/2}$–$^2P_{1/2}$ transition two orders larger than the contribution of the frequency-dependent part $[B(\omega)]$ whereas for $^2S_{1/2}$–$^2P_{3/2}$ transition, they are of the same order. The comparison of the results of Breit energies with those obtained by MBPT calculations [17] show small differences probably due to higher-order Breit contributions which are included in our calculations but not in MBPT.

Our calculations demonstrate the obvious need to include at least the frequency-independent Breit contribution together with the QED corrections in order to achieve good agreement with experiment in energy calculations for two- and three-electron systems. For not highly ionized systems like Ne^{+7} inclusion of only the Breit correction to the DC Hamiltonian may lead to worse transition energies as can be seen from Table IV. It could only improve the value of $^2P_{3/2}$–$^2P_{1/2}$ fine structure. For highly ionized systems like U^{+89} frequency-dependent Breit corrections are significant. Both the Breit interaction contributions and Lamb shift computed in this study agree favorably with those evaluated using other theoretical methods by different authors.

IV. SUMMARY AND CONCLUSIONS

In this work we have presented the scheme to generate of hydrogenic spin orbitals for the relativistic configuration interaction calculations. We have carried out a series of calculations of the correlation as well as relativistic effects in order to test the accuracy of this approach in comparison with other well-established methods.

The relativistic configuration interaction method using screened hydrogenic spin orbitals [RCI(SH)] yields for some two- and three-electron systems results comparable in accuracy to other accurate theoretical approaches. Particularly, the results allowing for Breit and QED corrections seem to be promising. The technique of construction of CSF space allows us to take correlation effects into account by using a relatively not very large basis set expansion. However, one can note that very high excited spin orbitals should be included in the basis set to calculate excited states (Table III). On the other hand, we can take advantage of the unique set of spin orbitals that can be used for all the states of the system studied. The obtained multiconfiguration wave functions are orthogonal, which is important if one assumes calculation of transition probabilities in the future.

The calculations presented here show that screened hydrogenic wave functions can be successfully used as spin orbitals in relativistic configuration interaction calculations. There are many advantages of using screened hydrogenic spin orbitals. They can be easily generated numerically or represented analytically. For the sake of convenience in this study we have used numerically generated wave functions, but many applications use analytical wave functions. They can be applied to the DCB Hamiltonian approach without any need of projection operators because such spin orbitals guarantee clean separation of negative and positive spectra.

ACKNOWLEDGMENTS

The authors kindly acknowledge the support of this study by the Pedagogical University of Cracow Research Grant.

---

[1] J. P. Desclaux, Comput. Phys. Commun. **9**, 31 (1975).
[2] I. P. Grant, B. J. McKenzie, P. H. Norington, D. F. Meyers, and N. C. Pyper, Comput. Phys. Comun. **21**, 207 (1980).
[3] L. Glowacki and J. Migdalek, J. Phys. B **36**, 3629 (2003).
[4] L. Głowacki, M. Stanek, and J. Migdalek, Phys. Rev. A **61**, 064501 (2000).
[5] L. Głowacki and J. Migdałek, Phys. Rev. A **80**, 042505 (2009).
[6] P. J. Mohr and Y. K. Kim, Phys. Rev. A **45**, 2727 (1992).
[7] D. Z. Kandula, C. Gohle, T. J. Pinkert, W. Ubachs, and K. S. E. Eikema, Phys. Rev. Lett. **105**, 063001 (2010).
[8] D. C. Morton, Q. Wu, and G. W. F. Drake, Can. J. Phys. **84**, 83 (2006).
[9] M. H. Chen, K. T. Cheng, and W. R. Johnson, Phys. Rev. A **47**, 3692 (1993).
[10] D. R. Plante, W. R. Johnson, and J. Sapirstein, Phys. Rev. A **49**, 3519 (1994).

[11] A. N. Artemyev, V. M. Shabaev, V. A. Yerokhin, G. Plunien, and G. Soff, Phys. Rev. A **71**, 062104 (2005).

[12] B. A. Bushaw, W. Nörtershauser, G. W. F. Drake, and H.-J. Kluge, Phys. Rev. A **75**, 052503 (2007).

[13] G. W. F. Drake, Can. J. Phys. **66**, 586 (1988).

[14] S. A. Blundell, W. R. Johnson, Z. W. Liu, and J. Sapirstein, Phys. Rev. A **40**, 2233 (1989).

[15] C. E. Moore, in *National Standard Reference Data Series*, NSRD-NBS 35 Vol. I, p. 359 (National Bureau of Standards, Washington, DC, 1971).

[16] M. H. Chen, K. T. Cheng, W. R. Johnson, and J. Sapirstein, Phys. Rev. A **52**, 266 (1995).

[17] S. A. Blundell, W. R. Johnson, and J. Sapirstein, Phys. Rev. A **41**, 1698 (1990).

[18] K. T. Cheng, M. H. Chen, and J. Sapirstein, Phys. Rev. A **62**, 054501 (2000).

[19] J. Schweppe, A. Belkacem, L. Blumenfeld, N. Claytor, B. Feinberg, H. Gould, V. E. Kostroun, L. Levy, S. Misava, J. R. Mowat *et al*., Phys. Rev. Lett. **66**, 1434 (1991).

[20] P. Beiersdorfer, D. Knapp, R. E. Marrs, S. R. Elliott, and M. H. Chen, Phys. Rev. Lett. **71**, 3939 (1993).

[21] S. A. Blundell, Phys. Rev. A **47**, 1790 (1993).

[22] V. A. Yerokhin, A. N. Artemyev, T. Beier, G. Plunien, V. M. Shabaev, and G. Soff, Phys. Rev. A **60**, 3522 (1999).